Journal Pre-proof

Chiral analysis of glycerol phosphates - Can bacteria biosynthesize heterochiral phospholipid membranes?

Andrea Palyzová , Irina A. Guschina , Tomáš Řezanka

Please cite this article as: Andrea Palyzová , Irina A. Guschina , Tomáš Řezanka , Chiral analysis of glycerol phosphates - Can bacteria biosynthesize heterochiral phospholipid membranes?, *Journal of Chromatography A* (2022), doi: https://doi.org/10.1016/j.chroma.2022.463267

Highlights

- Chiral HPLC was used to identify enantiomers of glycerolphosphates in four bacteria
- Phosphatidylglycerols were analyzed by LC/MS and by phospholipase C hydrolysis
- Bacteria contained two diacylglycerol enantiomers and may have heterochiral membranes
- Bacteria may synthesise both prokaryotic/eukaryotic and archaeal glycerolphosphates

Chiral analysis of glycerol phosphates - Can bacteria biosynthesize heterochiral phospholipid membranes?

Andrea Palyzová[1], Irina A. Guschina[2], Tomáš Řezanka[1✉]

[1] Institute of Microbiology, the Czech Academy of Sciences, 142 20 Prague 4, Czech Republic

[2] School of Biosciences, Cardiff University, Cardiff CF10 3AX, United Kingdom

T. Řezanka (✉)

e-mail: rezanka@biomed.cas.cz

Abstract

Phosphatidylglycerol (1,2-diacyl-*sn*-glycero-3-phospho-glycerol) (PG) is one of the most abundant lipids in bacteria. However, the chirality of the carbon atom on glycerol phosphate is different between the three kingdoms, Archaea, Bacteria, and Eukarya. Archaea membranes consist of phospholipids with glycerol-1-phosphate (G1P) in the *S* configuration, whereas phospholipids of the other two kingdoms contain glycerol-3-phosphate (G3P) having *R* stereochemistry. In the present study, GC/MS and LC/MS methods sensitively detected G3P and G1P from four bacterial strains (*Bacillus amyloliquefaciens*, *B. subtilis*, *Clavibacter michiganensis*, and *Geobacillus stearothermophilus*). Strain selection was carried out based on a GenBank search that revealed bacterial sequences associated with both enzymes involved in glycerol-phosphate synthesis, i.e., glycerol-3-phosphate dehydrogenase and glycerol-1-phosphate dehydrogenase. The detection of G1P and G3P was made by comparing the retention times of synthetic standards with those of analyzed samples. The structures of both glycerol phosphates were confirmed by selected ion monitoring (SIM) at *m/z* 171.006. The total concentration of G3P and G1P was around 30 μM, with a ratio of G3P to G1P of 4:1. We showed that PG was the most abundant phospholipid in all four bacteria by using the following analytical techniques and chromatographic modes: hydrophilic interaction liquid chromatography (HILIC), reversed-phase high-performance liquid chromatography high-resolution electrospray ionization tandem mass spectrometry (RP-HPLC/HR-ESI tandem MS) in negative and positive ionization modes, and an enzymatic cleavage by phospholipase C. By using chiral chromatography, the presence of both enantiomers in the glycerol backbone of some molecular species of PG was revealed. These results allow us to conclude that the bacteria examined here produce both enantiomer glycerol phosphates.

Keywords: Enantiomeric separation; Glycerol phosphates; RP-HPLC/MS-ESI[+]; Bacteria; Heterochiral membranes

Introduction

Membrane phospholipids of all living cells, from microorganisms to flowering plants and mammals, have a chiral atom in the glycerol backbone. The chirality of this carbon atom at glycerol-phosphate is different between Archaea and bacteria (Prokaryotes), and Eukaryotes. While Archaea membranes are formed of glycerol-1-phosphate (G1P) backbones having the *S* configuration, bacteria and Eukaryotes contain glycerol-3-phosphate (G3P) backbones having the *R* stereochemistry (Fig. 1). Archaea and bacteria have been hypothesized to originate from the Last Universal Common Ancestor (LUCA) suggesting the existence of a typical living ancestor in accordance to the common hypothesis of the origin of the three domains of life (Archaea, Bacteria, and Eukaryotes).

The common hypothesis of the origin of the three domains of life (Archaea, Bacteria, and Eukaryotes) suggests the existence of a typical living ancestor, known as the Last Universal Common Ancestor (LUCA), from which Archaea and bacteria originated. The differentiation of Archaea and bacteria is perceived in their membrane lipid distinguished chemical and physiological characteristics. Archaea lipids consist of branched isoprenoids linked by an ether bond to glycerol-1-phosphate (G1P), whereas phospholipids of bacteria and Eukaryotes contain fatty acids (FAs), which are ester-linked to the enantiomer, glycerol-3-phosphate (G3P). Although insignificant amounts of ether lipids and fatty acids ester-linked phospholipids were found in several bacteria and archaea, respectively, only a small amount of evidence for the coexistence of appreciable levels of the two phospholipid enantiomers as a hybrid heterochiral membrane in living bacterial cells have been demonstrated. For instance, Caforio and co-workers reported the engineering of *E. coli* by introducing membranes that were a hybrid of isoprenoids and fatty acids as well as heterochiral, since these lipids consisted of either a G1P or G3P backbone [1]. The bacterial cells, accumulated up to 30% of such lipids, were viable and the cell robustness towards variable growth conditions increased [1]. Lipids having both the *R* and *S* configurations on the glycerol phosphate backbone have been identified in our recent study [2]. It must be noted that, the determination how homochirality of biopolymers could have originally occurred is a long-standing scientific problem. It has been proposed that the first chiral supramolecular structures were micelles, vesicles, coacervates, etc., and the chirality of RNA, proteins, and other biopolymers arose after such structures had emerged [3,4]. Along with this, the question why Archaea biosynthesize *sn*-glycerol-1-phosphate, while bacteria and Eukaryotes synthesize *sn*-glycerol-3-phosphate, received no convincing answer.

The recent GenBank database search for sequences of the genes encoded glycerol-3-phosphate dehydrogenase (G3PDH), a key enzyme in G3P synthesis, revealed 623,000 corresponding sequences in bacteria. It is worth noting that the sequences associated with glycerol-1-phosphate dehydrogenase (G1PDH) involved in G1P synthesis, as believed exclusively in Archaea, were also found in about 14,000 searches in the GenBank database for bacteria. Hence, we assumed that the synthesis of G1P occurs in bacteria. Although these two enzymes catalyze the same reaction, namely the reduction of dihydroxyacetone phosphate (DHAP) using NADH (or NADPH) and divalent ions as cofactors (Fig. 2) [2,5], their sequences are not identical. Moreover, they do not have structural homology [6,7]. Since G1PDH has been detected in *Bacillus subtilis* [8], it may be suggested that this enzyme is not exclusively present in Archaea.

Separation and quantification of phosphorylated compounds, including glycerol esters with phosphoric acid as intermediates in carbon metabolism, is laborious because G3P or G1P are enantiomers. HPLC, GC, or capillary electrophoresis coupled with mass spectrometry have been used for G3P and G1P separation although with some limitations [9–14]. A proper separation of sugar phosphates and phosphate of hydroxy-carboxylic acids in biological samples by LC-MS was troublesome, because the high polarity of phosphorylated compounds lead to the low retention times (tR) when using the reversed-phase. In addition, a need to remove the ion-pairing agent salt is demanding. GC-MS can be effectively used to separate the anionic metabolites (after derivatization), since capillary columns have many theoretical plates and, therefore, provide an excellent resolution of many compounds. The combination of capillary electrophoresis with MS allowed the separation of four metabolites, i.e., glyceraldehyde-3-phosphate, glycerol-3-phosphate, dihydroxyacetone phosphate, and 3-phosphoglyceric acid, but the chirality of glycerol phosphates has not been achieved [13]. However, none of the published methodology/techniques has dealt with the separation and identification of G3P and G1P using the same column.

Another approach is to analyze the final products of biosynthesis, i.e., phospholipids. In addition to classical methodologies, hydrophilic interaction liquid chromatography (HILIC) and an identification by reversed-phase high-performance liquid chromatography-tandem mass spectrometry (RP-HPLC/MS/MS), the phospholipid analyses require an enzymatic cleavage by phospholipases C or chiral chromatography. In HILIC, lipids are separated based on the structure of the polar head groups. At the same time, the separation according to the chain length, a number, and configuration of double bonds, etc., is only partial. In contrast, lipids are separated by RP-HPLC according to the length and unsaturation of the hydrocarbon

chains . Lipid enantiomers can also be separated and identified by chiral chromatography [15].

All four bacteria, i.e., *Bacillus amyloliquefaciens, B. subtilis, Clavibacter michiganensis,* and *Geobacillus stearothermophilus*, contain monounsaturated fatty acids in small amounts (only a few percent of total FAs). In the Bacillaceae family, branched FAs from C15 to C17 were identified as the major patterns, with a predominance of odd FAs, i.e., ai-15:0, i-15:0, ai-17:0, i-17:0 and two even FAs (i-16:0 and 16:0) [15–20]. In the genus *Clavibacter* (phylum Actinobacteria, family Microbacteriaceae), saturated FAs were also prevalent, for example, ai-15:0 (44.9 %), i-16:0 (11.9 %), ai-17:0 (19.6 % of the total fatty acids) [21].

Phosphatidylethanolamine (PE) and phosphatidylglycerol (PG) have been detected as significant phospholipids of the most studied bacteria [23]. The presence of individual phospholipids, such as diphosphatidylglycerol (DPG, or cardiolipin) and PG in the genus *Clavibacter* [24], PE, PG and DPG in the family Bacillaceae, have been already revealed [19,21,25]. Dong and co-workers used matrix-assisted laser desorption/ionization time-of-flight mass spectrometry (MALDI-TOF) for lipidomic analysis of PE and PG isolated from *Geobacillus stearothermophilus* [25]. Several molecular species have been identified with the majority of 31:0, 32:0, 33:0, and 34:0 PG, where CN:DB described the ratio between carbon number and double bonds.

Oxygenated polyunsaturated fatty acids were separated by polysaccharide-based chiral stationary phases. Cellulose derivatives with tris(3,5-dimethylphenylcarbamate) showed the highest enantiomer resolution efficiency [26]. Triacylglycerols were also analyzed by multidimensional chromatography and mass spectrometry that allowed the separation of regioisomers and enantiomers. Triacylglycerols isolated from sea buckthorn have been reported to contain palmitic acid predominantly at the positions of *sn*-1 and/or *sn*-3 [27].

Based on the articles mentioned above and our previous papers describing the identification of regioisomers and enantiomers of various lipids [2,28], we analyzed PG from four bacteria which, according to the GenBank database, contained both enzymes, i.e. glycerol-3-phosphate dehydrogenase, and glycerol-1-phosphate dehydrogenase. The chosen strains were: *Bacillus amyloliquefaciens, B. subtilis, Clavibacter michiganensis,* and *Geobacillus stearothermophilus*. Using several analytical techniques, i.e., HILIC, RP-HPLC/HR-ESI tandem MS in negative and positive ionization modes, an enzymatic cleavage by phospholipase C and chiral chromatography, we showed that both glycerol-phosphate enantiomers were present in these bacteria. To provide more supportive evidence, diacyl

acetyl glycerols (AcTAGs) were prepared from the appropriate PGs. The final confirmation of the assumption that bacteria biosynthesize both G3P and G1P was made by using chiral chromatography. Given that the retention times of the analyzed samples from bacteria were in an accurate agreement with those of both standards (G3P and G1P) together with their mass spectra interpretation, the presence of two enantiomers of glycerol phosphates in the studied bacteria was thus proven.

2. Experimental methods

2.1. Chemicals and standards

sn-Glycerol-1-phosphate lithium salt, *sn*-glycerol-3-phosphate lithium salt, DL-α-glycerol phosphate magnesium salt hydrate, β-glycerol phosphate disodium salt pentahydrate, dihydroxyacetone phosphate dilithium salt, bis(monomyristoylglycero)phosphate (14:0/14:0-BMP (*S*,*R*)) (ammonium salt), 1,2-dipentadecanoyl-*sn*-glycero-3-phosphocholine, 1,2-dipentadecanoyl-*sn*-glycero-3-phospho-(1′-rac-glycerol) (sodium salt) (15:0/15:0-PG), 1,2-dimyristoyl-*sn*-glycero-3-phosphocholine (Cat. No. 850345), 2,3-dimyristoyl-*sn*-glycero-1-phosphocholine (Cat. No. 850857C) were purchased from Merck (previously Sigma-Aldrich, Prague, Czech Republic). All other chemical compounds and enzymes were also purchased from Merck.

2.2. Sample preparation of organisms

Four bacteria were cultured under standard conditions; see Supplements. Bacterial strains *Clavibacter michiganensis* (CCM 4974) and *Bacillus subtilis* were obtained from the Culture Collection of Microorganisms (Brno, Czech Republic), *Bacillus amyloliquefaciens* (DSM 23117) was obtained from DSMZ collection (Braunschweig, Germany), and *Geobacillus stearothermophilus* (ATCC 12980) from ATTC collection (Manasses, VA, USA). The cultures of bacteria were grown in minimal M9 medium (0.4% $(NH_4)_2SO_4$, 1.36% KH_2PO_4, 0.3% NaOH, 0.2% $MgSO_4 \times 7H_2O$, 0.02% $CaCl_2 \times 6H_2O$, 0.01% $FeSO_4 \times 7H_2O$, pH 7.2) supplemented with glucose (5 g/L; for all strains) and casein hydrolysate (10 g/L; for *Clavibacter michiganensis* and *Geobacillus stearothermophilus*). Cultures were incubated in 100 mL of a medium on an orbital shaker (190 rpm) for 24-48 h and at 30 °C or 56 °C (for strain *Geobacillus stearothermophilus*). *Saccharomyces pastorianus*, a bottom fermenting brewer's yeast, was obtained from a large brewery in the Czech Republic (yearly beer production of 130.000.000 L) [29].

2.3. Isolation of water-soluble metabolites

The method described by Bennett et al. [30] was used to extract water-soluble metabolites. Briefly, cells were extracted at -10 °C with acetonitrile: methanol: water with

0.1M formic acid (*v/v/v* 40:40:20), where formic acid is used for rapid and complete denaturation of proteins [31]. After 15 minutes of extraction, the cells were re-extracted, and the combined extracts were neutralized with ammonium hydroxide to prevent acid-catalyzed degradation of the metabolites.

2.4. Chiral LC-MS and GC-MS analysis of glycerol phosphates (G3P and G1P)

G3P and G1P were separated by an Astec cyclobond TM I 2000 DMP (3,5-dimethyl-phenyl-carbamate modified β-cyclodextrin) chiral LC column (5 μm, 25 cm × 4.6 mm) (Sigma-Aldrich, Prague, Czech Republic). The mobile phase consisted of a gradient from 95% A and 5% B at 0 min to 45% A and 55% B over 25 minfolows isocratically maintained for 5 min, where A was 5 mM ammonium formate (pH 4.0) and B was acetonitrile. The flow rate, column temperature, and injection volume were carried out 0.45 mL/min, 20 °C, and 10 μL, respectively. Detection was performed using an LTQ-Orbitrap Velos mass spectrometer in negative ESI mode. Glycerol phosphates were quantified by selected ion monitoring (SIM) of ion [M-H]$^-$ at *m/z* 171.006. The elution order of enantiomers from the chiral column was determined based on the t$_R$ of both commercially obtained standards and SIM. Quantification was based on comparison with standard calibration curves generated in the same manner.

Both commercially available standards, i.e. G3P and G1P (in concentration of 10 μM), were dissolved in acetonitrile:methanol:water with 0.1M formic acid (v/v/v 40:40:20). After 15 minutes, the solution was neutralized with ammonium hydroxide and analyzed by chiral LC-MS under the conditions described above. The results are shown in Figs. 1S and 2S.

Trimethylsilyl derivatives of both G3P and G1P were prepared by Nishihara and Koga [32]. Briefly, approximately 100 μL of the aqueous extract was derivatized with 0.8 mL of 1,1,1,3,3,3-hexamethyldisilazane (HMDS) and 0.4 mL of trimethylchlorosilane (TMCS). After completing the reaction (removing a large amount of water), 0.8 mL of HMDS and 0.4 mL of TMCS were added again. The solution was heated to 110 °C for 60 min. After cooling, the mixture was centrifuged at 10,000 rpm for 3 min, concentrated and analyzed by GC-MS.

GC-MS of silylated glycerophosphates (G3P and G1P) was done on a GC-MS system consisting of Varian 450 GC (Varian BVm Middleburg, Netherlands), Varian 240-MS ion trap detector with electron ionization (EI), and CombiPal autosampler (CTC, USA) equipped with split/splitless injector [29]. The sample was injected onto a 25 m × 0.25 mm × 0.1 um Ultra-1 capillary column (Supelco, Czech Republic) under a temperature program: 100 °C, increasing at 10 °C/min to 290 °C and 5 min at 290 °C. Helium was the carrier gas at a flow of 0.5 mL/min. Products were detected by selected ion monitoring for G3P or G1P (ions at *m/z* 357.1, 299.1, 73.0).

2.5. *Isolation of lipids*

Lipid extraction procedure was performed according to the Bligh and Dyer method [33] with modifications as previously described [34]. Dichlormethane and water were added after resuspending the lyophilized cells using the dichloromethane methanol mixture (2:1, *v/v*) for 30 min with stirring. The dichloromethane phase was evaporated to dryness under reduced pressure. For further analysis, total lipids were dissolved in the mobile phase (acetonitrile:2-propanol (99:1, *v/v*)).

2.6. *The semi-preparative HILIC-ESI-MS*

Semi-preparative HPLC equipment consisted of a 1090 Win system, a PV5 ternary pump (400 bar pressure (5801 psi)), an automatic injector (HP 1090 series, Hewlett Packard, USA), and HILIC HPLC ZIC®-HILIC 250 × 10 mm, 5 μm, 200Å column. An elution with a flow rate of 4.5 mL/min was performed and a linear gradient was carried out from the mobile phase containing methanol/acetonitrile/aqueous 1 mM ammonium acetate (50:30:20, *v/v/v*) to methanol/acetonitrile/aqueous 1 mM ammonium acetate (10:70:20, *v/v/v*) for 60 min. The column temperature was 35 °C and the re-equilibration period between runs was 30 min. The efficiency of the column was approximately 11,000 plates/25 cm. 1,2-Dipentanoyl-*sn*-glycero-3-phospho-(1′-rac-glycerol) (sodium salt) was used as an external standard. The eluent from the HPLC column was split so that 2% of the flow was introduced to ESI-MS, and 98% of the flow containing fractions of lipid classes were collected manually. The fraction of PG was further evaporated and redissolved in diethyl ether for enzymatic hydrolysis.

The LTQ-Orbitrap Velos mass spectrometer (Thermo Fisher Scientific, San Jose, CA, USA) was equipped with a heated electrospray interface (HESI) in positive and negative ionization modes. The MS scan range was performed in the FT cell and recorded within a window between 150–1000 *m/z*. The mass resolution was set to 105,000, and the ion spray voltage was set at -2.5/+3.5 kV in the positive/negative ionization mode. The ionization mode used the following parameters: N_2 was used as a nebulizer gas and set to 18 arbitrary units (sheath gas) and 7 arbitrary units (auxiliary gas); ion source temperature, 250 °C; capillary temperature, 230 °C; capillary voltage, 50 V; and tube lens voltage, 170 V. Helium was used as a collision gas for collision-induced dissociation (CID) experiments. The CID normalization energy of 35% was used for fragmentation of parent ions. The MS/MS product ions were detected in a high-resolution FT mode.

The MS spectrometer calibration was conducted using a Pierce LTQ Orbitrap positive and/or negative ion calibration solution (Thermo Fisher Scientific, San Jose, CA, USA). The

internal lock mass was used in mass spectra acquisition, i.e., 255.2330 m/z [M-H]$^-$ palmitic acid in the negative ESI. The mass accuracy was better than 1.0 ppm. The chemical structures of the compounds were confirmed with the help of the spectral database LIPID MAPS$^®$ Lipidomics Gateway (http://www.lipidmaps.org/).

2.7. Phospholipase C hydrolysis

The mixture of PGs collected in the interval 17.6 – 18.4 min (~ 1 mg) and commercially available *Bacillus cereus* phospholipase C (2.5 units) were dispersed in 1 mL of Tris buffer (17.5 mM; pH 7.3) with 1% calcium chloride (0.1 mL) and diethyl ether (0.3 mL) [35]. The mixture was shaken vigorously at 37 °C for approximately 45 min. TLC determined the degree of hydrolysis (silica gel with fluorescent indicator on 20 cm × 20 cm TLC plates (Merck, Prague, Czech Republic), mobile phase: dichloromethane-methanol-acetic acid (65:25:8, *v/v/v*)). The resulting glycerol derivatives were acetylated to acetyldiacylglycerols (AcTAGs) by standing overnight in a mixture of acetic anhydride/pyridine (3:2, *v/v*) at 20 °C [36].

2.8. Separation and identification of AcTAGs by RP-HPLC/tandem MS

The LC equipment consisted of a 1090 Win system, PV5 ternary pump and automatic injector (HP 1090 series, Agilent, Santa Clara, CA, USA) and three Luna Omega 1.6 μm, C18, 100 Å, LC Columns L × I.D. 150 × 2.1 mm, connected in series. 1,2-Dipentanoyl-3-acetyl-*sn*-glycerol with tR 661.2 min was used as an external standard, with a flow rate of 0.90 mL/min, an injection volume of 15 μL, and column temperature of 25 °C. The gradient program with the solvent mixture from 45% A (acetonitrile-2-propanol in ratio 1:1, *v/v*) and 55% B to 100% B (acetonitrile-2-propanol in ratio 2:3, *v/v*) was used. The composition was returned to the initial conditions for 20 min. The 10% HPLC flow was introduced into the ESI source, and 90% of the flow containing molecular species of AcTAGs was collected manually. The LTQ Orbitrap Velos was used under conditions as described above.

2.9. Pancreatic lipase hydrolysis, i.e., determination of fatty acids at the sn-2 position

Collected peak that was eluted in the interval 634.0 – 639.0 min and preliminarily identified as i-15:0/ai-15:0/2:0, pancreatic lipase (150 units), 150 μL Tris buffer, 25 μL sodium cholate (1 g/L), and 10 μL calcium chloride (2.2%) were mixed in a vial, heated at 40 °C for 1 min, and stirred for 2 min in a Vortex mixer. After cooling to 20 °C, 50 μL of 6 M HCl and 0.2 mL of diethyl ether were added. The reaction mixture was extracted with 0.2 mL diethyl ether three times. The combined ether extracts were separated by TLC (silica gel with fluorescent indicator on 20 cm × 20 cm TLC plates), mobile phase: hexane/diethyl ether/acetic acid (60:39:1, *v/v/v*). The bands corresponding to free fatty acids (FFAs) and

monoacylglycerols (*sn*-2 MAGs) were scraped from the plates, eluted from silica gel with diethyl ether and evaporated to dryness. *sn*-2 MAGs were transesterified to FAMEs as described previously [34]. FAMEs were prepared from FFAs using BF_3 in methanol [35].

2.10. Chiral analysis of AcTAGs by HPLC-ESI-tandem MS

The LC system used for separation in the chiral mode was the same as that used in the reversed-phase mode. AcTAGs (~1 mg/mL in a mobile phase) were chromatographically separated on two Astec cyclobond TM I 2000 DMP (3,5-dimethyl-phenyl-carbamate modified β-cyclodextrin) chiral LC columns (5 μm, 25 cm × 4.6 mm) (Sigma-Aldrich, Prague, Czech Republic) connected in series. The mobile phase was a gradient from 95% A and 5% B at 0 min to 45% A and 55% B over 180 min, and then isocratically maintained for 30 min, where A was hexane and B was a hexane-2-propanol (97:3, *v/v*) mixture [2,28]. The flow rate, column temperature, and injection volume were 0.45 mL/min, 24 °C, and 10 μL, respectively. As described above, other conditions were the same as those used for RP-HPLC/tandem MS. The two enantiomeric diacylglycerols obtained by hydrolysis by phospholipase C of commercially available standards (1,2-dimyristoyl-*sn*-glycero-3-phosphocholine and 2,3-dimyristoyl-*sn*-glycero-1-phosphocholine) were also acetylated, and the resulting triacylglycerols (1,2-dimyristoyl-3-acetyl-*sn*-glycerol and 2,3-dimyristoyl-3-acetyl-*sn*-glycerol) were used as external standards. Additional information/details on this analysis can be found in our previous publications [39–41].

3. Results and discussion

3.1. Extraction and analysis of glycerol phosphates (G3P and G1P)

The cells were extracted (twice) at -10 °C with 0.1M formic acid (formic acid is required for rapid and nearly complete denaturation of proteins) [31]. The extract was neutralized with ammonium hydroxide to prevent acid-catalyzed degradation of the metabolites. The extract was separated on a chiral column (Astec cyclobond TM I 2000 DMP; 5 μm, 25 cm × 4.6 mm). Both glycerol phosphates (G3P and G1P) were analyzed in a negative ESI mode by monitoring of ion [M-H]⁻ at *m/z* 171.006. The identification was performed based on the similarity of retention times of both synthetic standards with those of analyzed samples and SIM at *m/z* 171.006. Quantification was performed using a calibration curve obtained using synthetic standards. Fig. 3 shows four chromatograms of synthetic mixtures where the ratio of G3P to G1P was 1:1 (20 μM + 20 μM), 4:1 (10.0 μM + 2.5 μM), 10:1 (4.0 μM + 0.4 μM) 40:1 (1.0 μM + 0.025 μM), in parentheses are the concentrations of both glycerol phosphates injected onto the column. Furthermore, all four bacteria and yeast were analyzed. Only G3P was identified in the yeast, or if G1P was present, its concentration

would have to be less than 0.01 μM based on the calibration curve determination. The analysis of all four bacteria gave different results. In all cases, the G1P concentrations ranged from 5 to 12 μM and the G3P concentrations ranged from 23 to 34 μM. These results show that the ratio G3P/G1P was approximately 3:1 to 4:1 for all four bacteria (Table S1).

The stability of individual enantiomers, i.e. G3P and G1P, was confirmed by chiral LC-MS. Both Figs. 1S and 2S showed that there is only a slight isomerization of phosphoryl group transfer during at least 45 minutes. For G3P, the amount of the enantiomer decreased from 97.5% to 95.2% (Fig. 1S). For G1P, the amount of the enantiomer decreased from 96.3% to 94.4% (Fig. 2S). Thus, it is conceivable to suppose that isomerization was almost inappreciable during the extraction and analytical procedure (chiral LC-MS)

Intracellular metabolite concentrations of G3P in glucose-fed, exponentially growing *E. coli* have been shown to be around 4.9×10^{-5} mol/L (which is 49 μM) [30]. This value is comparable to our values being around 30 μM for all four bacteria (Table S1). The minor differences can be explained by the fact that all four bacteria used in this study are Gram-positive bacteria, in contrast to *E. coli*, which is a Gram-negative bacterium. In yeast *S. pastorianus*, eukaryotic cells, a concentration similar to bacteria was found, i.e., about 25 μM/L. The published data on G3P concentration in yeast *Spathaspora arborariae* under aerobic cultivation [42] are similar to our findings: 7.58 μg/mL (44 μM), whereas the lower concentration of G3P (2.61 μg/mL ≈ 15 μM) was found under oxygen-limited conditions.

. Our GC-MS analyses showed that the decomposition of both phosphates was not more significant than the relative 5%. Unfortunately, about 50% of both G3P and G1P were degraded in the bacterial extracts within 24 hrs at 20 °C. We suggest that it is most likely due to incomplete denaturation of the enzymes involved in such degradation of bacterial extracts as noted previously by Rabinowitz and Kimball [31]. The stability of metabolites, including G3P, stored at room temperature, has been described in urine samples [43]. In those samples, Glycerol-3-phosphate was almost stable for 28 days, then its concentration reduced by about 10% during the longer storage. In contrast, Bajad and co-workers reported that G3P belongs to a group of unstable compounds or could not be measured for other reasons in *E. coli*. [41]. The stability of phosphorylated compounds has been investigated by Nam and co-workers [13]. They found that, except for two metabolites (glyceraldehyde-3-phosphate (GA3P) and dihydroxyacetone phosphate (DHAP)), all other studied metabolites, including G3P, were stable in either freeze-thaw cycles or in the samples exposure to -80 °C for 30 days.

3.2. Analysis of fatty acids

Individual samples from four bacteria (see Experimental) were lyophilized and extracted according to the method of Bligh and Dyer [33] using a phospholipase-inactivating modification step [34]. Total FAs were esterified and further analyzed as fatty acid methyl esters (FAMEs) by GC-MS. The differences between straight-chain (normal), iso, and anteiso FAs were revealed based on the identity of FAME retention times between the standards (*sn*-glycerol-1-phosphate lithium salt, *sn*-glycerol-3-phosphate lithium salt) and analyzed samples of four bacteria, as well as based on the mass spectra of 3-pyridylcarbinyl esters (see below). Based on identification by retention times (tR) of standards (Bacterial Acid Methyl Ester (BAME) Mix, Merck) and mass spectra, see below, it was suggested that the studied bacteria contain predominantly branched-chain FAs (Figs. 3S, 4S, and 5S). This was fully confirmed by the mass spectra of 3-pyridylcarbinyl esters (formerly picolinyl esters) by means of GC-MS. Ions at m/z 92 and m/z 108 are present in the mass spectrum of all 3-pyridylcarbinyl esters of FAs . The spectrum of 3-pyridylcarbinyl ester of i-15:0 is similar to that of a straight-chain saturated pentadecanoic 3-pyridylcarbinyl ester except for a very clear gap of 28 Da between ions at m/z 290 and m/z 318, representing the loss of C14 methyl group and its attached methyl group, which definitely locates it. The remaining ions are evenly spaced 14 Da gaps. In the mass spectrum of 3-pyridylcarbinyl methyltetradecanoate (ai-15:0), this gap of 28 Da is shifted between ions at m/z 276 and 304. These findings are fully confirmed by already published papers [45,46].

3.3. Hydrophilic interaction liquid chromatography - HILIC

The lipid class profile of four bacteria were analyzed by HILIC; Fig. 4 shows the data. Separation of diacyl standards of BMP, PG and DPG was easily achieved, and phospholipid classes were separated at the baseline. The separation time using a semi-preparative column with a diameter of 10 mm was from 15 to 21 mins. A number of different classes of phospholipids are shown in Table 2. The preliminary PG structure was determined based on tR compared to standards. The PG fraction was collected manually and further analyzed by RP-HPLC/MS after hydrolysis by phospholipase C and derivatization to give AcTAGs (see below).

BMPs represent a different structural variation of PGs in the *sn* position of fatty acid chains. While PGs have acyls in position *sn*-1, *sn*-2, then BMPs have acyls in the *sn*-1, *sn*-1' position [47]. Since PGs and BMPs have the same sum formula, they cannot be distinguished by MS level. Tandem MS, which in the negative ion mode can confirm the structures of fatty acid chains, seems more promising. Yet still it cannot clearly distinguish PG from BMP. Therefore, PG and BMP were analyzed both in the negative ion mode (to identify fatty acid

chains) and in the positive ion mode (to identify *sn* position of fatty acid chains). Protonated molecular ions provided completely different tandem mass spectra of PG and BMP, with PG producing diacylglycerols ions and BMP producing monoacylglycerols ions [48]. In this study, molecular species of 15:0/15:0-BMP provides fragment ions at *m/z* 397.2352 and *m/z* 379.2246, corresponding to a loss of FA chain (Fig. 6S). Due to head group loss, tandem MS of isomorphic molecular species 15:0/15:0-PG produced a protonated fragment ion at *m/z* 523.4725 (Fig. 6S). In negative tandem high resolution, mass spectrum of the major molecular species, i.e. 15:0/15:0-PG. Briefly, in tandem MS, abundant ions were resulted from a loss of *sn*-1 and *sn*-2 acyl chains as ketene (RCH=C=O) from [M-H]$^-$ at *m/z* 469.2573 or a neutral loss of *sn*-1 and *sn*-2 RCOOH group from [M-H]$^-$ at *m/z* 451.2468. Other ions were also identified, i.e. a precursor ion [M-H]$^-$ (693.4713 Da), *sn*-1 and *sn*-2 RCOO$^-$ (241.2174 Da), and glycerophosphoglycerol ion with H_2O loss at *m/z* 227.0328, etc.

This HILIC approach allowed us to separate PG and BMP. The structure of the major molecular species of DPG, i.e. 15:0/15:0-15:0/15:0-DPG is provided in our previous paper [2]. PG was found as the prevalent phospholipid in *B. subtilis* [49], and a molecular species 30:0-PG was the most abundant phospholipid in the *B. subtilis* strain DSM 3257 [50]. Further, Shah et al. [51] identified 15:0/15:0-PG with *m/z* 693.4712 in thermophilic *Geobacillus* sp. (strain GWE1) as one of the major phospholipids. Considering the published data and the results obtained in the present study, we confirmed that PG is the principal phospholipid in all four bacteria. Therefore, it was selected for further analysis.

3.4. Analysis of AcTAGs by RP-HPLC

In the next step of the analysis, the HILIC fraction (i.e., PG manually collected in the separation time range of 17.6 - 18.4 min) was hydrolyzed with phospholipase C. The obtained 1,2-diacyl-*sn*-glycerols were immediately derivatized to AcTAGs to prevent acyl migration during subsequent separation processes. Based on our analysis of FAMEs and the published data [47,48] see above, it could be assumed that the most molecular species will contain branched fatty acids. Therefore, gradient elution was used for RP-HPLC analysis. Using this gradient elution, three major molecular species containing branched acids were separated on the baseline, namely i-15:0/i-15:0/2:0, i-15:0/ai-15:0/2:0 (or ai-15:0/i-15:0/2:0), and ai-15:0/ai-15:0/2:0 (Fig. 5). The identification and other characteristics of twenty-one molecular species are listed in Table 1. The structure of the mixed product, i-15:0/ai-15:0/2:0 and/or ai-15:0/i-15:0/2:0, respectively, was confirmed after its hydrolysis by pancreatic lipase, which selectively hydrolyzes FAs on the primary hydroxyls of glycerol (position *sn*-1 and/or *sn*-3). The resulting mixture of free FAs and 2-monoacylglycerols was separated by TLC as

previously described [28]. After esterification and transesterification, respectively, FAMEs (i-15:0 and ai-15:0) were determined by GC-MS. It was found that molecular species with tR 634.0 – 639.0 min, are more than 90% consisted of i-15:0/ai-15:0/2:0. After collection of AcTAGs, two molecular species containing either i-15:0 or only ai-15:0 were separated by chiral chromatography.

Tandem MS of ammonium adduct at m/z 600.5200 ([M+NH$_4$]$^+$) produced two most abundant ions, i.e. [DAG]$^+$ ions. These ions ([M+H-FA]$^+$) arise a neutral loss of acetic acid+NH$_4$ from [M+H]$^+$ at m/z 523.4723 and pentadecanoic acid+NH$_4$ from [M+H]$^+$ at m/z 341.2688. Additional ions that confirm the structure AcTAG, i.e. 15:0/15:0/2:0, were identified. They are four ions at m/z 299.2582 (*sn*-1 or *sn*-2 acyl chain ([RC=O+74]$^+$)), m/z 281.2476 (*sn*-1 or *sn*-2 acyl chain ([RC=O+74]$^+$) loss of H$_2$O)), m/z 225.2214 *sn*-1 or *sn*-2 acyl chain ([RC=O]$^+$), and m/z 207.2108 (*sn*-1 or *sn*-2 acyl chain ([RC=O-H$_2$O]$^+$). Another pair of TAGs containing branched FAs, i.e. i-15:0 and/or ai-15:0, has a completely identical tandem MS (as indicated by FAMEs analysis by GC-MS).

Twenty-four molecular species were identified in *B. licheniformis*, with the largest abundances being 30:0-PG (15:0/15:0 and/or 14:0/16:0) and 32:0-PG (15:0/17:0 and/or 16:0/16:0) [52]. Molecular species at m/z 693.3, i.e. dipentadecanoyl-PG, was also dominant, approximately 60% of the base peak, in *G. stearothermophilus* [25].

Although Lopes et al. [52] concluded that: "It is not possible to distinguish the linear C15 and C17 from their branched isomers by LC-MS and MS/MS analysis" (the authors described the molecular species of phospholipids, mainly PG and PE), we were able to separate three molecular species of C15/C15/2:0 mainly due to the reduction of the polarity of the analyzed compounds. The polar head (glycerol-3-phosphate) has been removed, and separation of three molecular species of C15/C15/2:0-TAGs differing only in branched chains was successful.

3.5. Analysis of bacteria by chiral HPLC

Furthermore, chiral HPLC (Fig. 6) was used to analyze AcTAG, obtained in a similar manner to that previously published [2]. Briefly, individual AcTAGs, i.e. two peaks separated by RP-HPLC and collected in the intervals 611.0 – 616.0 and 654.0 – 659.0 min, respectively, were separated into enantiomers. The two standards, 1,2-di-myristoyl-3-acetyl-*sn*-glycerol and 2,3-di-myristoyl-1-acetyl-*sn*-glycerol, were prepared (see Experimental). Based on the retention times of both synthetic enantiomers, the elution order from the chiral column was determined. The *R* enantiomer elutes first. The ratio of *R* and *S* enantiomers of natural PGs was approximately 1:3 to 1:4, which is fully consistent with the results of G1P and G3P chiral

chromatography. Further analysis showed that AcTAGs of four bacteria were mixtures of *R* and *S* enantiomers with almost identical tandem mass spectra (Fig. 7). It was found that the *S* enantiomer of AcTAG was predominant, meaning that the *R* enantiomer was present in PG (Fig. 8). This figure shows the uses of the Cahn-Ingold-Prelog rule. It should be noted that although the configuration on carbon 2 of glycerol is the same, due to the rule (different counting of the order of atoms), the *R* and *S* descriptions are changed.

Our suggestion that bacteria of four chosen genera may use two pathways for synthesis of G3P and G1P was based on the results of the GenBank database search (Tables S2 and 3). This search shows that both enzymes, glycerol-3-phosphate dehydrogenase (G3PDH) and glycerol-1-phosphate dehydrogenase (G1PDH), are present in these bacteria. The structure of glycerol-1-phosphate dehydrogenase in *B. subtilis* has been published 15 years ago [53]. Conversely, proteins with G3PDH activity have been identified in Archaea [54], e.g., in strains of *Archaeoglobus veneficus*, *Methanobrevibacter oralis*, *Haloterrigena thermotolerans,* etc. It is noteworthy, that more than 4200 other strains of Archaea were determined in the GenBank database (access date February 3, 2022) which contain a protein with G3PDH activity.

Conclusions

The generally accepted hypothesis [55] about the diversity of membrane composition distinguishing Archaea from bacteria and Eukarya is that Archaea contain G1P as a head group in the membrane phospholipids, whereas bacteria and Eukaryotes contain in membranes its enantiomer, G3P [56]. There are many hypotheses about the origin of life on Earth, or more to the point, of the existence of a common living ancestor, noted as LUCA (last universal common ancestor). In 2003, Wächtershäuser theorized [57] that LUCA membrane phospholipids were heterochiral. A widely accepted earlier statement that lipids of different chirality are incompatible, and that two lipid enantiomers are unstable led to the lipid separation or "lipid divide" theory [54]. Since then, many researchers have challenged this theory. The stereo specificity of archaeal lipids and their unique structures were hypothesized to be more chemically stable and heat resistant, but this has been called into questions by a number of studies. It has been shown that heterochiral membranes were as stable or even more stable than homochiral membranes [58]. A recent study has demonstrated their resilience to environmental stresses [1]. Furthermore, *E. coli* was used as a model system for expressing archaeal lipids in the bacterial cell membrane [1]. The amount of 20-30% of archaeal lipids in the bacterial cell made it possible to analyze their effect on the mixed membrane cell's organism. While growth was unchanged, then the robustness of the cells with

a hybrid heterochiral membrane was slightly increased. Thus, such findings contrasted the hypothesis of the thermodynamic instability of mixed membranes. The Fibrobacteres-Chlorobi-Bacteroidetes group, found deep in the Black Sea, was possibly the first group of organisms identified with the ability to synthesize a heterochiral membrane [59].

One of the most direct pieces of evidence has been reported 25 years ago, when it was demonstrated that *E. coli* contained PG having *R*, *S* and *R*, *R* diastereoisomers [60]. In this case, it is a "side chain" of glycerol, i.e. glycerol to which an ester bond does not bind acyls, but both enantiomers of glycerol should still be synthesized.

Our results convincingly proved that the four analyzed bacteria have heterochiral membranes. Chiral chromatography of both glycerol phosphates and analysis of PG in the form of AcTAGs demonstrated that both enantiomers of glycerol phosphates are present in the cells. Although their concentrations can be determined very roughly, the analysis suggests that the content of the less represented *S* enantiomer (according to the previous theories, bacteria cannot synthesize it) reached 20-30% of the *R* enantiomer level. This finding follows from the data shown in Fig. 3 (chiral chromatography G3P and G1P) and Fig. 6 (chiral chromatography of diacyl acetyl glycerols). This level of enantiomer accumulation is in agreement with the mentioned above results on the genetically modified *E. coli*, where the introduction of 20-30% of archaeal lipids in cell membranes did not affect the cell viability [1].

More research is needed in this direction with further studies of lipids in various bacteria and Archaea to confirm the hypothesis of heterochiral membranes in these organisms.

Acknowledgments

References

[1]   A. Caforio, M.F. Siliakus, M. Exterkate, S. Jain, V.R. Jumde, R.L.H. Andringa, S.W.M. Kengen, A.J. Minnaard, A.J.M. Driessen, J. van der Oost, Converting *Escherichia coli* into an archaebacterium with a hybrid heterochiral membrane, PNAS 115 (2018) 3704–3709. https://doi.org/10.1073/PNAS.1721604115.

[2]   M. Vítová, M. Stránská, A. Palyzová, T. Řezanka, Detailed structural characterization of cardiolipins from various biological sources using a complex analytical strategy comprising fractionation, hydrolysis and chiral chromatography, J. Chromatogr. A 1648 (2021) 462185. https://doi.org/10.1016/J.CHROMA.2021.462185.

[3]   K. Ikehara, Possible steps to the emergence of life: the [GADV]-protein world hypothesis, Chem. Rec. 5 (2005) 107–118. https://doi.org/10.1002/TCR.20037.

[4]   D. Deamer, The role of lipid membranes in life's origin, Life (Basel) 7 (2017). https://doi.org/10.3390/LIFE7010005.

[5]   J.S. Han, K. Ishikawa, Active site of Zn(2+)-dependent sn-glycerol-1-phosphate dehydrogenase from *Aeropyrum pernix* K1, Archaea 1 (2005) 311–317. https://doi.org/10.1155/2005/257264.

[6]   Y. Koga, H. Morii, Biosynthesis of ether-type polar lipids in Archaea and evolutionary considerations, Microbiol. Mol. Biol. Rev. 71 (2007) 97–120. https://doi.org/10.1128/MMBR.00033-06.

[7]   J. Lombard, P. On L´Opez-García, D. Moreira, Phylogenomic investigation of phospholipid synthesis in Archaea, Archea 2012 (2012) 13. https://doi.org/10.1155/2012/630910.

[8]   H. Guldan, F.M. Matysik, M. Bocola, R. Sterner, P. Babinger, Functional assignment of an enzyme that catalyzes the synthesis of an Archaea-type ether lipid in bacteria, Angew. Chem. Int. Ed. 50 (2011) 8188–8191. https://doi.org/10.1002/ANIE.201101832.

[9]   J.M. Buescher, S. Moco, U. Sauer, N. Zamboni, Ultrahigh performance liquid chromatography-tandem mass spectrometry method for fast and robust quantification of anionic and aromatic metabolites, Ana.l Chem. 82 (2010) 4403–4412. https://doi.org/10.1021/AC100101D.

[10]   B. Luo, K. Groenke, R. Takors, C. Wandrey, M. Oldiges, Simultaneous determination of multiple intracellular metabolites in glycolysis, pentose phosphate pathway and tricarboxylic acid cycle by liquid chromatography-mass spectrometry, J. Chromatogr. A 1147 (2007) 153–164. https://doi.org/10.1016/J.CHROMA.2007.02.034.

[11]   W. Lu, M.F. Clasquin, E. Melamud, D. Amador-Noguez, A.A. Caudy, J.D. Rabinowitz, Metabolomic analysis via reversed-phase ion-pairing liquid chromatography coupled to a stand alone orbitrap mass spectrometer, Anal. Chem. 82 (2010) 3212–3221. https://doi.org/10.1021/AC902837X.

[12]   C. Cipollina, A. ten Pierick, A.B. Canelas, R.M. Seifar, A.J.A. van Maris, J.C. van Dam, J.J. Heijnen, A comprehensive method for the quantification of the non-oxidative pentose phosphate pathway intermediates in *Saccharomyces cerevisiae* by GC-IDMS, J. Chromatogr. B Analyt. Technol. Biomed. Life Sci. 877 (2009) 3231–3236. https://doi.org/10.1016/J.JCHROMB.2009.07.019.

[13]   M. Nam, M.S. Kim, G.S. Hwang, Optimization and validation of capillary electrophoresis- and gas chromatography-tandem mass spectrometry methods for the analysis of intermediate metabolites in glycolysis and pentose phosphate pathways within biological samples, J. Chromatogr. A 1656 (2021). https://doi.org/10.1016/J.CHROMA.2021.462531.

[14]   M.M. Koek, B. Muilwijk, M.J. van der Werf, T. Hankemeier, Erratum: Microbial metabolomics with gas chromatography/mass spectrometry, Anal. Chem. 78 (2006) 3839. https://doi.org/10.1021/AC060521Q.

[15]   T. Rezanka, I. Kolouchova, A. Cejkova, T. Cajthaml, K. Sigler, Identification of regioisomers and enantiomers of triacylglycerols in different yeasts using reversed- and chiral-phase LC-MS, J. Sep. Sci. 36 (2013) 3310–3320. https://doi.org/10.1002/jssc.201300657.

[16] T. Kaneda, Positional distribution of fatty acids in phospholipids from *Bacillus subtilis*, Biochim. Biophys. Acta. 270 (1972) 32–39. https://doi.org/10.1016/0005-2760(72)90174-9.

[17] T. Kaneda, Fatty acids of the genus Bacillus: an example of branched-chain preference, Bacteriol. Rev. 41 (1977) 391–418. https://doi.org/10.1128/BR.41.2.391-418.1977.

[18] H. lin Zhu, G. Chen, S. ni Chen, R. qi Wang, L. Chen, H. Xue, S. ping Jian, Changes in cell membrane properties and phospholipid fatty acids of *Bacillus subtilis* induced by polyphenolic extract of Sanguisorba officinalis L, J. Food Sci. 85 (2020) 2164–2170. https://doi.org/10.1111/1750-3841.15170.

[19] J.C. Paton, B.K. May, W.H. Elliott, Membrane phospholipid asymmetry *in Bacillus amyloliquefaciens*, J. Bacteriol. 135 (1978) 393–401. https://doi.org/10.1128/JB.135.2.393-401.1978.

[20] L. Siristova, K. Melzoch, T. Rezanka, Fatty acids, unusual glycophospholipids and DNA analyses of thermophilic bacteria isolated from hot springs, Extremophiles 13 (2009) 101–109. https://doi.org/10.1007/S00792-008-0202-6.

[21] A. Coorevits, A.E. Dinsdale, G. Halket, L. Lebbe, P. de Vos, A. van Landschoot, N.A. Logan, Taxonomic revision of the genus *Geobacillus*: emendation of *Geobacillus*, *G. stearothermophilus, G. jurassicus, G. toebii, G. thermodenitrificans* and *G. thermoglucosidans* (nom. corrig., formerly '*thermoglucosidasius*'); transfer of *Bacillus thermantarcticus* to the genus as *G. thermantarcticus* comb. nov.; proposal of *Caldibacillus debilis* gen. nov., comb. nov.; transfer of *G. tepidamans* to *Anoxybacillus* as *A. tepidamans* comb. nov.; and proposal of *Anoxybacillus caldiproteolyticus* sp. nov, Int. J. Syst. Evol. Microbiol. 62 (2012) 1470–1485. https://doi.org/10.1099/IJS.0.030346-0.

[22] S.W. Liu, F.N. Li, H.Y. Zheng, X. Qi, D.L. Huang, Y.Y. Xie, C.H. Sun, *Planctomonas deserti* gen. nov., sp. nov., a new member of the family Microbacteriaceae isolated from soil of the Taklamakan desert, Int. J. Syst. Evol. Microbiol. 69 (2019) 616–624. https://doi.org/10.1099/IJSEM.0.003095.

[23] C. Sohlenkamp, O. Geiger, Bacterial membrane lipids: diversity in structures and pathways, FEMS Microbiol. Rev. 40 (2016) 133–159. https://doi.org/10.1093/FEMSRE/FUV008.

[24] P. Schumann, P. Kämpfer, H.J. Busse, L.I. Evtushenko, Proposed minimal standards for describing new genera and species of the suborder Micrococcineae, Int. J. Syst. Evol. Microbiol. 59 (2009) 1823–1849. https://doi.org/10.1099/IJS.0.012971-0.

[25] W. Dong, Q. Shen, J.T. Baibado, Y. Liang, P. Wang, Y. Huang, Z. Zhang, Y. Wang, H.Y. Cheung, Phospholipid analyses by MALDI-TOF/TOF mass spectrometry using 1,5-diaminonaphthalene as matrix, Int. J. of Mass Spectrom. 343–344 (2013) 15–22. https://doi.org/10.1016/J.IJMS.2013.04.004.

[26] F. Ianni, G. Saluti, R. Galarini, S. Fiorito, R. Sardella, B. Natalini, Enantioselective high-performance liquid chromatography analysis of oxygenated polyunsaturated fatty acids, Free Radic. Biol. Med. 144 (2019) 35–54. https://doi.org/10.1016/J.FREERADBIOMED.2019.04.038.

[27] M. Kalpio, K.M. Linderborg, M. Fabritius, H. Kallio, B. Yang, Strategy for stereospecific characterization of natural triacylglycerols using multidimensional chromatography and mass spectrometry, J. Chromatogr. A 1641 (2021) 461992. https://doi.org/10.1016/J.CHROMA.2021.461992.

[28] A. Palyzová, T. Cajthaml, T. Řezanka, Separation of regioisomers and enantiomers of triacylglycerols containing branched fatty acids (iso and/or anteiso), Electrophoresis 42 (2021). https://doi.org/10.1002/ELPS.202000320.

[29] T. Řezanka, I. Kolouchová, L. Gharwalová, A. Palyzová, K. Sigler, Identification and characterization of phospholipids with very long chain fatty acids in brewer's yeast, Lipids 52 (2017) 1007–1017. https://doi.org/10.1007/S11745-017-4294-6.

[30] B.D. Bennett, E.H. Kimball, M. Gao, R. Osterhout, S.J. van Dien, J.D. Rabinowitz, Absolute metabolite concentrations and implied enzyme active site occupancy in *Escherichia coli*, Nat. Chem. Biol. 5 (2009) 593–599. https://doi.org/10.1038/NCHEMBIO.186.

[31] J.D. Rabinowitz, E. Kimball, Acidic acetonitrile for cellular metabolome extraction from *Escherichia coli*, Anal. Chem. 79 (2007) 6167–6173. https://doi.org/10.1021/AC070470C.

[32] M. Nishihara, Y. Koga, Gas-liquid chromatographic determination of total glycerophosphate in an aqueous solution, Anal. Biochem. 276 (1999) 260–261. https://doi.org/10.1006/ABIO.1999.4370.

[33] E.G. BLIGH, W.J. DYER, A rapid method of total lipid extraction and purification, Can. J. Biochem. Physiol. 37 (1959) 911–917. https://doi.org/10.1139/O59-099.

[34] M. Kates, B.E. Volcani, Biosynthetic pathways for phosphatidylsulfocholine, the sulfonium analogue of phosphatidylcholine, in Diatoms, In: Kiene R.P., Visscher P.T., Keller M.D., Kirst G.O. (eds) Biological and Environmental Chemistry of DMSP and Related Sulfonium Compounds, Springer, Boston, MA. (1996) 109–119. https://doi.org/10.1007/978-1-4613-0377-0_10.

[35] K. Yokota, R. Kanamoto, M. Kito, Composition of cardiolipin molecular species in *Escherichia coli*, J. Bacteriol. 141 (1980) 1047–1051. https://doi.org/10.1128/jb.141.3.1047-1051.1980.

[36] Y. Xu, P.A. Siegenthaler, Phosphatidylglycerol molecular species of photosynthetic membranes analyzed by high-performance liquid chromatography: theoretical considerations, Lipids 31 (1996) 223–229. https://doi.org/10.1007/BF02522624.

[37] W.W. Christie, Xianlin. Han, Lipid analysis : isolation, separation, identification and lipidomic analysis, 4th ed, The Oily Press: Bridgwater UK, (2010) 428. https://books.google.com/books/about/Lipid_Analysis.html?hl=cs&id=XaggBQAAQBAJ (accessed February 8, 2022).

[38] A. Vančura, T. Řezanka, J. Maršlálek, K. Melzoch, G. Basařová, V. Křišťan, Metabolism of L-threonine and fatty acids and tylosin biosynthesis in Streptomyces fradiae, FEMS Microbio. Lett. 49 (1988) 411–415. https://doi.org/10.1111/j.1574-6968.1988.tb02767.x.

[39] Y. Itabashi, J.J. Myher, A. Kuksis, Determination of positional distribution of short-chain fatty acids in bovine milk fat on chiral columns, J. Am. Oil Chem. Soc. 70 (1993) 1177–1181. https://doi.org/10.1007/BF02564223.

[40] J.K. Limb, Y.H. Kim, S.Y. Han, G.J. Jhon, Isolation and characterization of monoacetyldiglycerides from bovine udder, J. Lipid Res. 40 (1999) 2169–2176. https://doi.org/10.1016/S0022-2275(20)32091-5.

[41] P. Kalo, A. Kemppinen, V. Ollilainen, A. Kuksis, Regiospecific determination of short-chain triacylglycerols in butterfat by normal-phase HPLC with on-line electrospray-tandem mass spectrometry, Lipids 39 (2004) 915–928. https://doi.org/10.1007/S11745-004-1314-3.

[42] C.G. Campos, H.C.T. Veras, J.A. de Aquino Ribeiro, P.P.K.G. Costa, K.P. Araújo, C.M. Rodrigues, J.R.M. de Almeida, P.V. Abdelnur, New protocol based on UHPLC-MS/MS for quantitation of metabolites in xylose-fermenting yeasts, J. Am. Soc. Mass Spectrom. 28 (2017) 2646–2657. https://doi.org/10.1007/S13361-017-1786-9.

[43] X.W. Fu, M. Iga, M. Kimura, S. Yamaguchi, Simplified screening for organic acidemia using GC/MS and dried urine filter paper: a study on neonatal mass screening, Early Hum. Dev. 58 (2000) 41–55. https://doi.org/10.1016/S0378-3782(00)00053-0.

[44] S.U. Bajad, W. Lu, E.H. Kimball, J. Yuan, C. Peterson, J.D. Rabinowitz, Separation and quantitation of water soluble cellular metabolites by hydrophilic interaction chromatography-tandem mass spectrometry, J. Chromatogr. A 1125 (2006) 76–88. https://doi.org/10.1016/J.CHROMA.2006.05.019.

[45] W.W. Christie, Gas chromatography-mass spectrometry methods for structural analysis of fatty acids, Lipids 33 (1998) 343–353. https://doi.org/10.1007/S11745-998-0214-X.

[46] D.J. Harvey, Picolinyl esters as derivatives for the structural determination of long chain branched and unsaturated fatty acids, Biomed. Mass Spectrom. 9 (1982) 33–38. https://doi.org/10.1002/BMS.1200090107.

[47] S. Czolkoss, P. Borgert, T. Poppenga, G. Hölzl, M. Aktas, F. Narberhaus, Synthesis of the unusual lipid bis(monoacylglycero)phosphate in environmental bacteria, Environ. Microbiol. 23 (2021) 6993–7008. https://doi.org/10.1111/1462-2920.15777.

[48] J.A. Hankin, R.C. Murphy, R.M. Barkley, M.A. Gijón, Ion mobility and tandem mass spectrometry of phosphatidylglycerol and bis(monoacylglycerol) phosphate (BMP), Int. J. Mass Spectrom. 378 (2015) 255–263. https://doi.org/10.1016/J.IJMS.2014.08.026.

[49] A.Y. van Tilburg, P. Warmer, A.J. van Heel, U. Sauer, O.P. Kuipers, Membrane composition and organization of *Bacillus subtilis* 168 and its genome-reduced derivative miniBacillus PG10, Microb. Biotechnol. (2021). https://doi.org/10.1111/1751-7915.13978.

[50] P. Bernat, K. Paraszkiewicz, P. Siewiera, M. Moryl, G. Płaza, J. Chojniak, Lipid composition in a strain of *Bacillus subtilis*, a producer of iturin A lipopeptides that are active against uropathogenic bacteria, World J. Microbiol. Biotechnol. 32 (2016). https://doi.org/10.1007/S11274-016-2126-0.

[51] S.P. Shah, S.A. Jansen, L.J.A. Taylor, P.L.G. Chong, D.N. Correa-Llantén, J.M. Blamey, Lipid composition of thermophilic *Geobacillus* sp. strain GWE1, isolated from sterilization oven, Chem. Phys. Lipids 180 (2014) 61–71. https://doi.org/10.1016/J.CHEMPHYSLIP.2014.02.005.

[52] C. Lopes, J. Barbosa, E. Maciel, E. da Costa, E. Alves, P. Domingues, S. Mendo, M.R.M. Domingues, Lipidomic signature of *Bacillus licheniformis* I89 during the different growth phases unravelled by high-resolution liquid chromatography-mass spectrometry, Arch. Biochem. Biophys. 663 (2019) 83–94. https://doi.org/10.1016/J.ABB.2018.12.024.

[53] H. Guldan, R. Sterner, P. Babinger, Identification and characterization of a bacterial glycerol-1-phosphate dehydrogenase: Ni(2+)-dependent AraM from *Bacillus subtilis*, Biochemistry 47 (2008) 7376–7384. https://doi.org/10.1021/BI8005779.

[54] A. Caforio, A.J.M. Driessen, Archaeal phospholipids: Structural properties and biosynthesis, Biochim. Biophys. Acta Mol. Cell Biol. Lipids 1862 (2017) 1325–1339. https://doi.org/10.1016/J.BBALIP.2016.12.006.

[55] H.S. Martin, K.A. Podolsky, N.K. Devaraj, Probing the role of chirality in phospholipid membranes, Chembiochem 22 (2021) 3148–3157. https://doi.org/10.1002/CBIC.202100232.

[56] S.I. Yokobori, Y. Nakajima, S. Akanuma, A. Yamagishi, Birth of Archaeal Cells: Molecular phylogenetic analyses of G1P dehydrogenase, G3P dehydrogenases, and glycerol kinase suggest derived features of Archaeal membranes having G1P polar lipids, Archaea 2016 (2016). https://doi.org/10.1155/2016/1802675.

[57] G. Wächtershäuser, From pre-cells to Eukarya--a tale of two lipids, Mol. Microbiol. 47 (2003) 13–22. https://doi.org/10.1046/J.1365-2958.2003.03267.X.

[58] H. Shimada, A. Yamagishi, Stability of heterochiral hybrid membrane made of bacterial sn-G3P lipids and archaeal sn-G1P lipids, Biochemistry 50 (2011) 4114–4120. https://doi.org/10.1021/BI200172D.

[59] L. Villanueva, F.A.B. von Meijenfeldt, A.B. Westbye, S. Yadav, E.C. Hopmans, B.E. Dutilh, J.S.S. Damsté, Bridging the membrane lipid divide: bacteria of the FCB group superphylum have the potential to synthesize archaeal ether lipids, ISME J. 15 (2021) 168–182. https://doi.org/10.1038/S41396-020-00772-2.

[60] Y. Itabashi, A. Kuksis, Reassessment of stereochemical configuration of natural phosphatidylglycerols by chiral-phase high-performance liquid chromatography and electrospray mass spectrometry, Anal. Biochem. 254 (1997) 49–56. https://doi.org/10.1006/ABIO.1997.2418.

Figures

Figure 1. The structure includes different nomenclature of glycerol-3-phosphate and glycerol-1-phosphate.
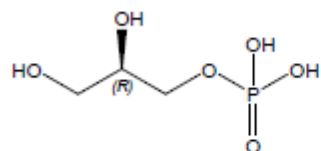
(R)-2,3-dihydroxypropyl dihydrogen phosphate
Chemical Formula: $C_3H_9O_6P$
Exact Mass: 172.0137
sn-Glycerol 3-phosphate
D-Glycerol 1-phosphate
L-Glycerol 3-phosphate
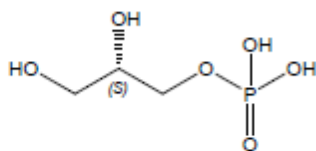
(S)-2,3-dihydroxypropyl dihydrogen phosphate
Chemical Formula: $C_3H_9O_6P$
Exact Mass: 172.0137
sn-Glycerol 1-phosphate
D-Glycerol 3-phosphate
L-Glycerol 1-phosphate

Figure 2. Biosynthesis of both enantiomers of glycerol-3-phosphate (in bacteria including Eukaryotes) and glycerol-1-phosphate (in Archaea).
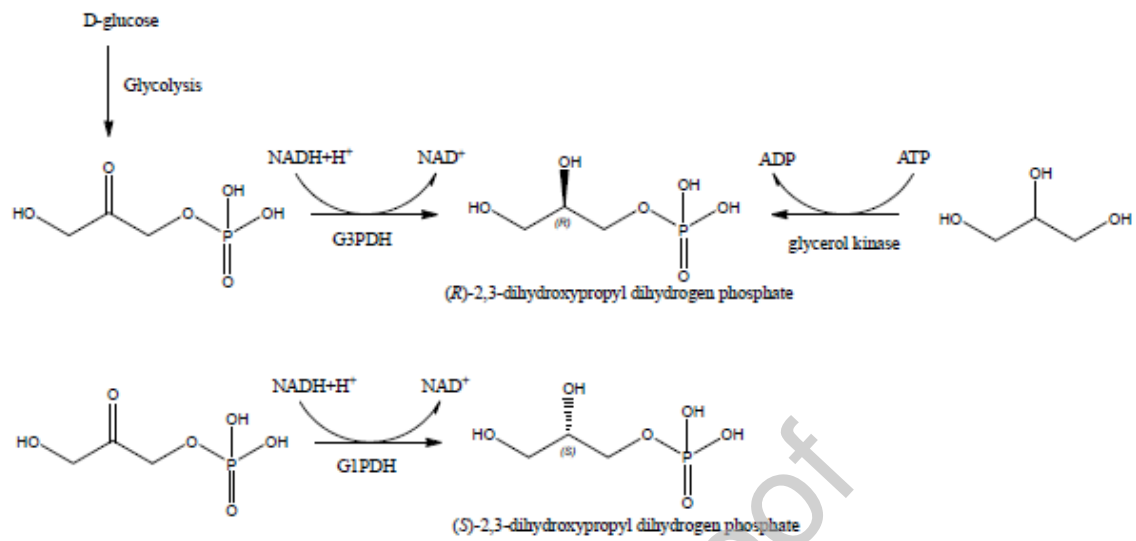
Figure 3. Four chromatograms of synthetic mixtures of G3P and G1P at different ratios and concentrations are shown. Further, five chromatograms of yeast and bacteria are presented. G3P and G1P were separated by an Astec cyclobond TM I 2000 DMP chiral LC column (5 μm, 25 cm × 4.6 mm). The gradient mobile phase was 5 mM ammonium formate (pH 4.0) and acetonitrile. Glycerol phosphates were quantified by selected ion monitoring (SIM) of ion [M-H]⁻ at m/z 171.006. The elution order of enantiomers from the chiral column was determined based on the tR of both commercially obtained standards and SIM.
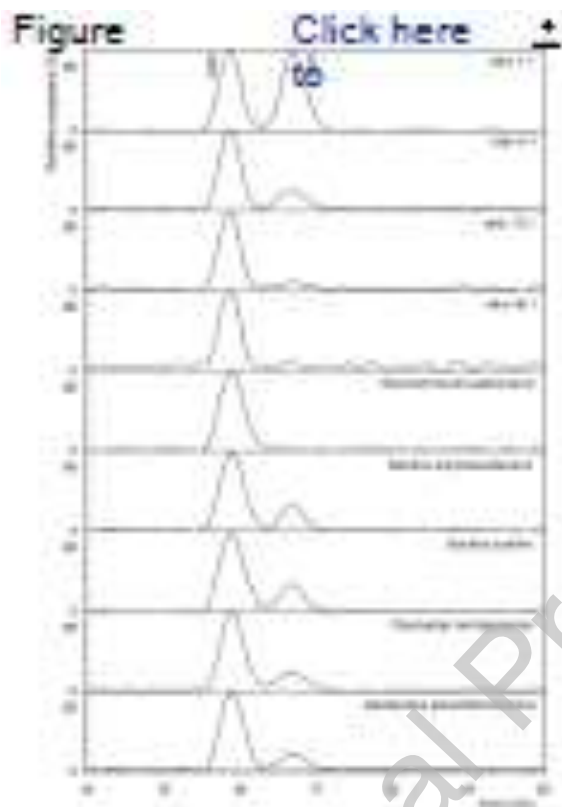
Figure 4. Hydrophilic interaction liquid chromatography - HILIC/ESI-MS separation of the major lipid classes of five microorganisms, i.e., four bacterial strains and yeast. Standards: bis(monoacylglycero)phosphate (BMP), phosphatidylglycerol (PG), and diphosphatidylglycerol (DPG). HILIC 250 × 10 mm × 5 μm column was used for semi-preparative HPLC, flow rate of 4.5 mL/min, gradient of the mobile phase containing methanol/acetonitrile/aqueous 1 mM ammonium acetate was used. The eluent from the HPLC column was split so that 2% of the flow was introduced to ESI-MS, and 98% of the flow containing fractions of lipid classes were collected manually.
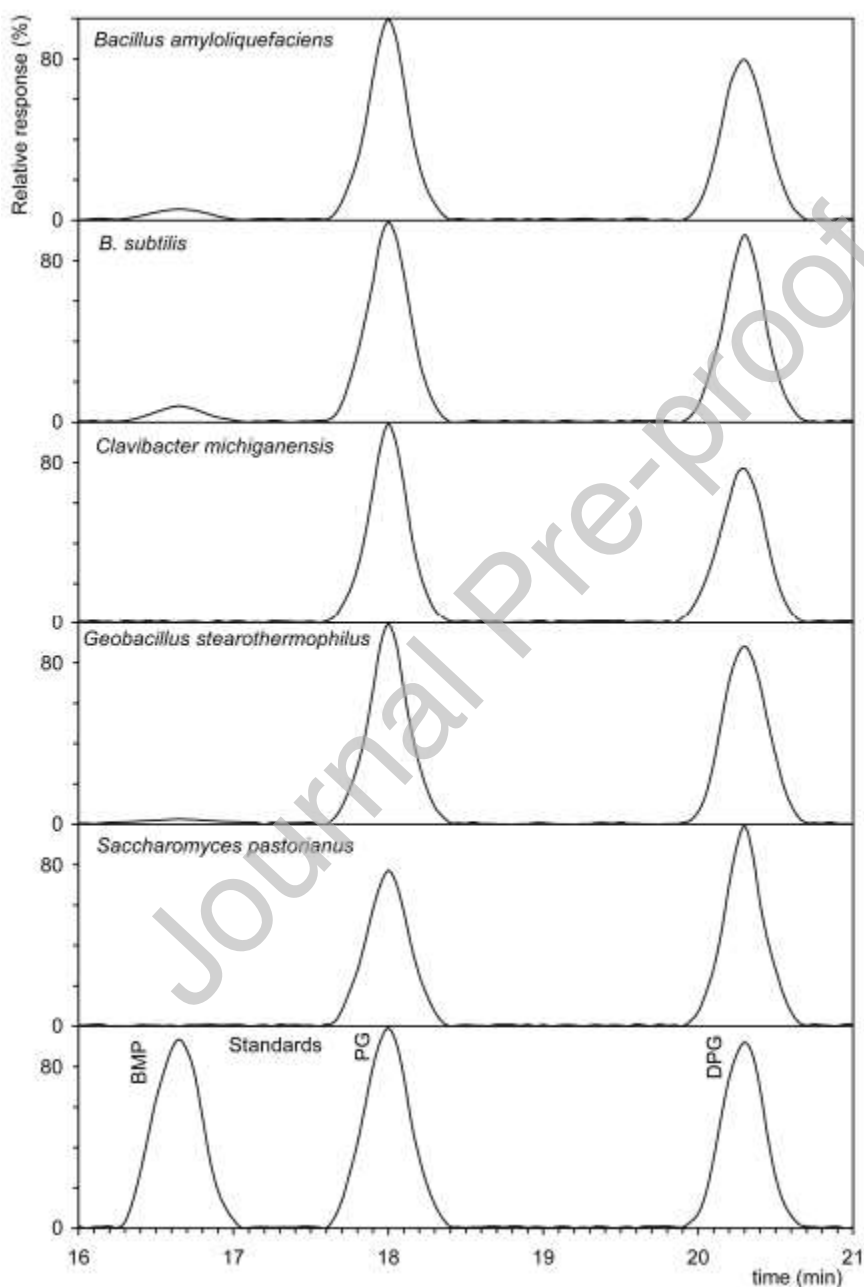
Figure 5. Separation of AcTAGs obtained after hydrolysis by phospholipase C from four bacteria. The total ion current was filtered and exhibited ions from 200 to 1500 Da. Numbers, see Table 1. Bold numbers - numbers that have been further identified. Three Luna Omega 1.6 μm, C18 columns L × I.D. 150 × 2.1 mm, connected in series was used with a flow rate of 0.90 mL/min. The gradient program from acetonitrile-2-propanol in ratio 1:1, **v/v** and acetonitrile-2-propanol in ratio 2:3, *v/v* was used. The 10% HPLC flow was introduced into the ESI source, and 90% of the flow containing molecular species of AcTAGs was collected manually.
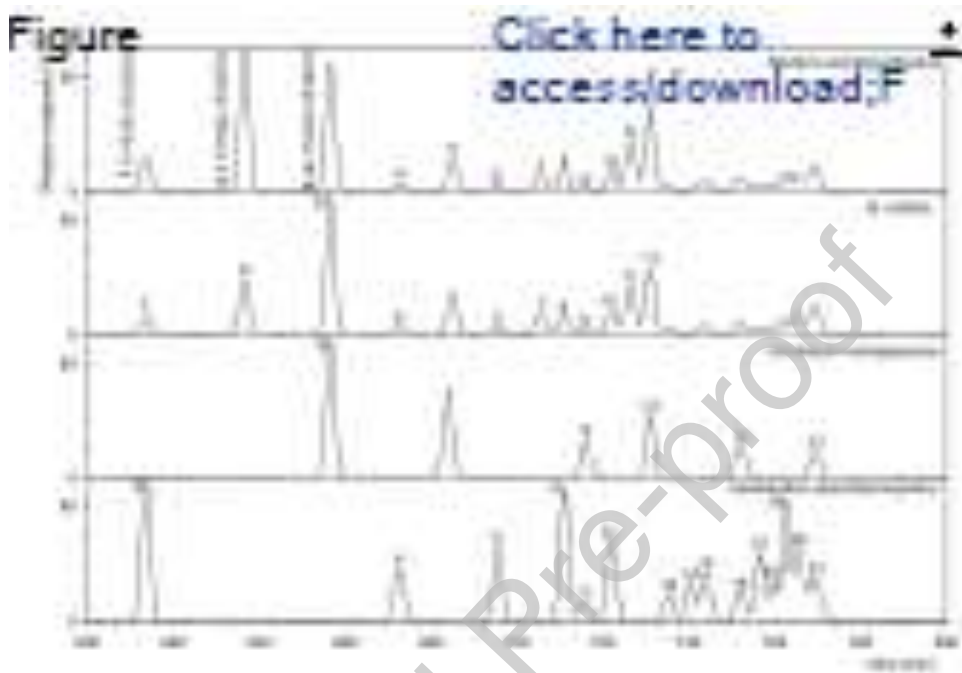
Figure 6. Chiral separation of natural AcTAG from four bacterial strain including synthesized internal standards (1,2-di-myristoyl-3-acetyl-*sn*-glycerol and 2,3-di-myristoyl-1-acetyl-*sn*-glycerol). Two Astec cyclobond TM I 2000 DMP 5 μm × 25 cm × 4.6 mm were connected in series. The mobile phase was a gradient hexane-2-propanol mixture, with flow rate 0.45 mL/min.

Figure 7. Tandem mass spectra of four isomers, two pairs of enantiomers (i-15:0/i-15:0/2:0, 2:0/i-15:0/i-15:0, ai-15:0/ai-15:0/2:0, and 2:0/ai-15:0/ai-15:0). For experimental details, see Experimental conditions and explanation of chromatographic behavior, in all figures, including mass spectra, see Results and Discussion.
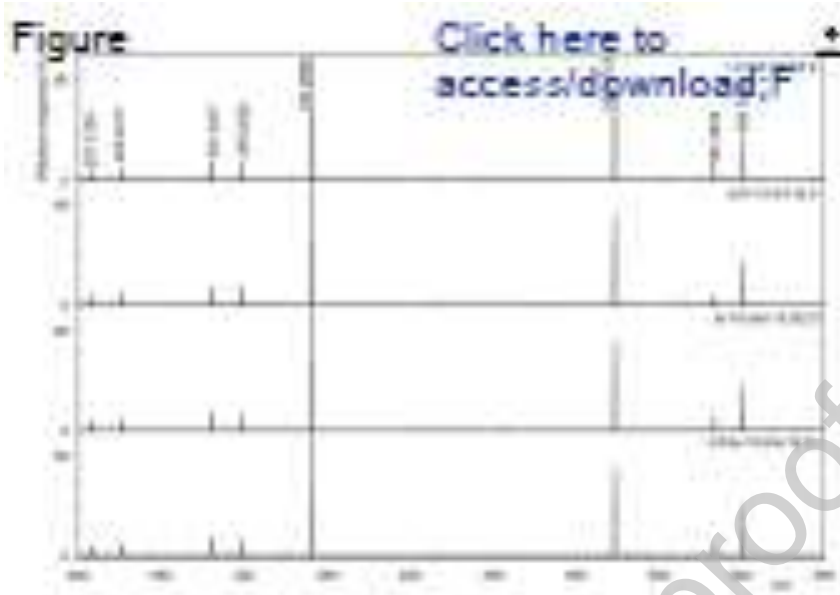
Figure 8. Use of the Cahn-Ingold-Prelog rule to determine the stereochemistry of PG and AcTAGs, respectively.

(2R)-3-[[(2,3-dihydroxypropoxy)(hydroxy)phosphoryl)oxy]
propane-1,2-diyl bis(13-methyltetradecanoate)
R-G3P lipid

(2S)-3-[[(2,3-dihydroxypropoxy)(hydroxy)phosphoryl)oxy]
propane-1,2-diyl bis(13-methyltetradecanoate)
S-G1P lipid

(S)-3-acetoxypropane-1,2-diyl bis(13-methyltetradecanoate)

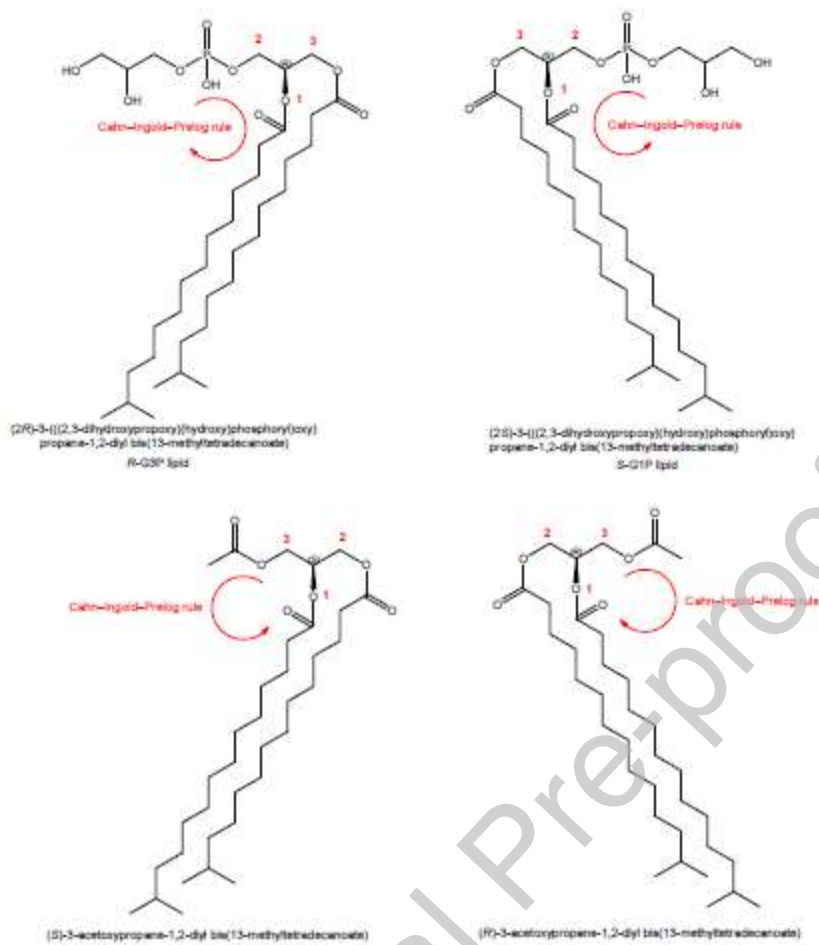(R)-3-acetoxypropane-1,2-diyl bis(13-methyltetradecanoate)

Table 1. Identification of molecular species of AcTAGs from four bacteria [a]

Peak No.	tR (min)	mol spec	*Bacillus amyloliquefaciens*	*B. subtilis*	*Clavibacter michiganensis*
1	613.6	i-15:0/i-15:0/C2:0	5.1 ± 0.3[b]	3.6 ± 0.2	0 ± 0
2	636.6	i-15:0/ai-15:0/C2:0	21.6 ± 1.7	9.5 ± 1.1	0 ± 0
3	656.8	ai-15:0/ai-15:0/C2:0	19.3 ± 0.9	25.4 ± 1.2	37.9 ± 1.6
4	672.4	i-15:0/i-16:0/C2:0	1.3 ± 0.1	1.9 ± 0.2	0 ± 0
5	684.2	ai-15:0/i-16:0/C2:0	5.1 ± 0.4	5.1 ± 0.4	19.7 ± 1.9
6	695.6	i-15:0/C16:0/C2:0	1.1 ± 0.2	1.4 ± 0.3	0 ± 0
7	705.6	ai-15:0/C16:0/C2:0	2.7 ± 0.3	3.8 ± 0.3	0 ± 0
8	711.2	i-15:0/i-17:0/C2:0	3.1 ± 0.2	3.3 ± 0.4	0 ± 0
9	716.2	i-16:0/i-16:0/C2:0	0.6 ± 0.1	1.0 ± 0.1	10.3 ± 2.0
10	722.0	i-15:0/ai-17:0/C2:0	3.2 ± 0.3	4.3 ± 0.6	0 ± 0
11	726.4	ai-15:0/i-17:0/C2:0	7.9 ± 1.6	8.9 ± 0.5	0 ± 0
12	731.2	ai-15:0/ai-17:0/C2:0	12.3 ± 1.4	11.2 ± 1.8	16.4 ± 1.4
13	735.8	i-16:0/C16:0/C2:0	0.6 ± 0.1	0.7 ± 0.2	0 ± 0
14	740.4	C16:0/C16:0/C2:0	0.5 ± 0.1	0.6 ± 0.1	0 ± 0
15	744.2	i-16:0/i-17:0/C2:0	1.6 ± 0.4	1.8 ± 0.3	0 ± 0
16	752.0	i-16:0/ai-17:0/C2:0	2.0 ± 0.3	2.3 ± 0.4	8.6 ± 1.7
17	756.4	C16:0/i-17:0/C2:0	1.0 ± 0.1	1.3 ± 0.1	0 ± 0
18	760.2	C16:0/ai-17:0/C2:0	1.4 ± 0.3	1.7 ± 0.2	0 ± 0
19	762.8	i-17:0/i-17:0/C2:0	2.9 ± 0.4	3.1 ± 0.3	0 ± 0
20	765.6	i-17:0/ai-17:0/C2:0	2.8 ± 0.6	4.0 ± 0.2	0 ± 0
21	769.6	ai-17:0/ai-17:0/C2:0	3.9 ± 0.8	5.1 ± 0.6	7.1 ± 0.9

[a] abundance (relative %)

[b] Mean ± S.D. from three measurements, i.e. relative %.

Table 2. The abundance of different classes of phospholipids

Bacterium	bis(monoacylglycero)phosphates	phosphatidylglycerols	diphosphatidylglycerols
Bacillus amyloliquefaciens	3.9	50.8	45.3
B. subtilis	4.7	49.7	45.6
Clavibacter michiganensis	0.7	52.2	47.1
Geobacillus stearothermophilus	2.2	49.1	48.7
Saccharomyces pastorianus	0.7	45.9	53.4

Declaration of Competing Interest

The authors declare that they have no conflict of interest.

Andrea Palyzová: Cultivation of bacteria, Analysis, Data curation, Methodology, Writing.

Irina A. Guschina: Data curation, Methodology, Writing- Original draft preparation.

Tomáš Řezanka: Analysis, Conceptualization, Software, Writing- Reviewing and Editing, Supervision.